



Assessment of TanDEM-X DEM 2020 Data in Temperate and Boreal Forests and Their Application to Canopy Height Change

Michael Schlund¹  · Felicitas von Poncet² · Birgit Wessel³ · Barbara Schweisshelm⁴ · Nadine Kiefl⁵

Received: 14 December 2022 / Accepted: 13 February 2023
© The Author(s) 2023

Abstract

Space-borne digital elevation models (DEM) are considered as important proxy for canopy surface height and its changes in forests. Interferometric TanDEM-X DEMs were assessed regarding their accuracy in forests of Germany and Estonia. The interferometric synthetic aperture radar (InSAR) data for the new global TanDEM-X DEM 2020 coverage were acquired between 2017 and 2020. Each data acquisition was processed using the delta-phase approach for phase unwrapping and comprise an absolute height calibration. The results of the individual InSAR heights confirmed a substantial bias in forests. This was indicated by a mean error (ME) between -5.74 and -6.14 m associated with a root-mean-squared-error (RMSE) between 6.99 m and 7.40 m using airborne light detection and ranging (LiDAR) data as a reference. The bias was attributed to signal penetration, which was attempted to be compensated. The ME and RMSE improved substantially after the compensation to the range of -0.54 to 0.84 m and 3.55 m to 4.52 m. Higher errors of the penetration depth compensated DEMs compared to the original DEMs were found in non-forested areas. This suggests to use the penetration compensation only in forests. The potential of the DEMs for estimating height changes was further assessed in a case study in Estonia. The canopy height change analysis in Estonia indicated an overall accuracy in terms of RMSE of 4.17 m and ME of -0.93 m on pixel level comparing TanDEM-X and LiDAR height changes. The accuracy improved substantially at forest stand level to an RMSE of 2.84 m and an ME of -1.48 m. Selective penetration compensation further improved the height change estimates to an RMSE of 2.14 m and an ME of -0.83 m. Height loss induced by clearcutting was estimated with an ME of -0.85 m and an RMSE of 3.3 m. Substantial regrowth resulted in an ME of -0.46 m and an RMSE of 1.9 m. These results are relevant for exploiting multiple global acquisitions of TanDEM-X, in particular for estimating canopy height and its changes in European forests.

Keywords InSAR · TanDEM-X · Canopy height changes · LiDAR · Forest

1 Introduction

The climate-driven increase in forest disturbances, such as fires, wind throws, and insect infestations, in the last decades affected the vulnerability of European forests reducing their carbon storage potential (Forzieri et al. 2021; Seidl et al. 2014). Furthermore, forests play an important role as carbon sinks. In this context, the spatial and temporal information about aboveground biomass (AGB) as a proxy for forest carbon stocks and its dynamics is relevant for estimating the global carbon balance (GCOS 2015; Pan et al. 2011), but also for quantifying forest vulnerability (Forzieri et al. 2021).

The calibration of individual AGB estimates to quantify temporal changes remains a challenge leading to large uncertainties in the estimation of AGB changes (Araya et al. 2022; Herold et al. 2019). Alternatively, forest canopy height

✉ Michael Schlund
m.schlund@utwente.nl

¹ Faculty of Geo-Information Science and Earth Observation, University of Twente, Enschede, The Netherlands

² Intelligence, Airbus Defence & Space, Immenstaad, Germany

³ German Remote Sensing Data Center, German Aerospace Center (DLR), Oberpfaffenhofen, Germany

⁴ Remote Sensing Technology Institute, German Aerospace Center (DLR), Oberpfaffenhofen, Germany

⁵ Bayerische Staatsforsten AöR, Munich, Germany

changes derived from, for example, global interferometric synthetic aperture radar (InSAR) digital elevation models (DEM) have been proposed as an accurate predictor for estimating AGB changes (Solberg et al. 2018; Karila et al. 2019; Schlund et al. 2021). In addition to AGB, the heterogeneity of forest canopy heights is assumed to be one of the most important proxies for ecosystem complexity and for predicting biodiversity (Atkins et al. 2021; Feng et al. 2020; Gatti et al. 2017). Consequently, canopy height is considered as an Essential Biodiversity Variable (EBV) that can be estimated using earth observation techniques (Skidmore et al. 2021).

Light detection and ranging (LiDAR) height measurements are recognised as the most accurate source for estimating forest canopy height as the difference between surface and terrain height. Nevertheless, their limited extent and high costs are prohibitive for repeated acquisitions over large areas (Koch 2010; Coops et al. 2021). Airborne or spaceborne optical stereo imaging systems also have the potential to create digital surface models (DSM) as a proxy of forest canopy surface height. For instance, DSMs from high-resolution optical sensors, such as ALOS/PRISM, Cartosat-1, and RapidEye, were regarded as suitable to monitor the vertical structure of forests (Tian et al. 2017). However, optical systems are constrained by weather conditions and cloud cover resulting potentially in temporal inconsistencies and data gaps (Tian et al. 2017; Ullah et al. 2020).

In contrast, the TanDEM-X InSAR system is able to deliver large scale gap-free coverages at high resolution independent from cloud cover. The primary mission goal was the production of a global DEM, which was finalised in 2016 and is considered as consistent and very accurate (Rizzoli et al. 2017; Wessel et al. 2018). The InSAR data to create this DEM were acquired between the years 2010 and 2014 (Rizzoli et al. 2017). In the years 2017–2020, an additional global coverage of InSAR data was acquired (Lachaise et al. 2020; Wessel et al. 2022). These data are used to produce a new global DEM, the so-called TanDEM-X DEM 2020 (formerly named ChangeDEM), which, together with the first acquisition period, could provide a basis for forest canopy height change estimation.

Despite the short wavelength of the X-band sensors and the corresponding scattering in the higher canopy, various studies suggested a high potential of TanDEM-X to retrieve forest structure information (Karila et al. 2015, 2019; Abdullahi et al. 2016; Sadeghi et al. 2016). This is based mostly on the assumption that X-band penetrates little into the vegetation and, therefore, the derived DSM represents the height of the forest canopy surface. For instance, the TanDEM-X DEM was combined with terrain height to obtain a canopy height model (CHM) that could be further related to AGB (Karila et al. 2015; Solberg et al. 2017; Schlund et al. 2020). However, a substantial penetration and resulting negative bias of TanDEM-X

InSAR heights was frequently observed in forests (Kugler et al. 2014; Sadeghi et al. 2016; Schlund et al. 2019a). Empirical models using a reference terrain or canopy height (e.g., from LiDAR), tree cover, or other external variables were used to estimate accurate canopy height from TanDEM-X (Sadeghi et al. 2016; Solberg et al. 2018; Ullah et al. 2020). However, the penetration depth can also be estimated without the need of external calibration data (Schlund et al. 2019a). This estimation method can be used to provide unbiased and more accurate forest canopy heights (Schlund et al. 2019a, 2021; Wang et al. 2021).

Using multi-temporal InSAR acquisitions from SRTM and TanDEM-X to derive changes in the forest canopy surface height proved to be very useful to detect clearcutting and other sources of deforestation in European forests (Solberg et al. 2013; Gdulová et al. 2021). Further, the changes in the canopy surface height in boreal and tropical forests were related to temporal changes in AGB (Solberg et al. 2018; Karila et al. 2019; Schlund et al. 2021). Note that the change in canopy surface height is independent of the terrain information. The information on height change has to date mainly been used to determine the spatial extent of forest changes and the relationship to AGB. The quantitative height change itself from TanDEM-X DEMs in forests has been under-explored so far. In addition, several global TanDEM-X InSAR coverages have only been available for a few years, and thus, an assessment of their quality with respect to the global TanDEM-X DEM 2020 has not yet been performed.

Consequently, the objective of this study is to evaluate the quality of the TanDEM-X InSAR heights over forest recorded during the global TanDEM-X DEM 2020 acquisition. Furthermore, the potential of combining TanDEM-X InSAR heights from the two global acquisition periods to derive forest canopy heights and their changes on regional scale is assessed. In the first part of this study, we focus our analysis on three different study areas in European forests. The InSAR heights' accuracy with and without penetration bias compensation is assessed. This is not only relevant for accurate canopy height estimation, in areas where digital terrain models (DTM) are available, e.g., from preceding laser scanning campaigns or other national surveys, but also in terms of error propagation for a subsequent InSAR height change assessment. Hence, in the second part of this study, a case study of the accuracies of the change in forest canopy height (ΔH) from TanDEM-X is performed. The information on changes is evaluated at both pixel and stand level in an Estonian forest site, distinguishing between different types of changes, such as forest clearcutting, regrowth, and more subtle changes caused by forest management operations. Therefore, this study provides relevant findings in the exploitation of multiple global acquisitions from TanDEM-X.

The structure of this paper reflects the division of the study into the aforementioned two parts, the TanDEM-X DEM 2020 validation and the forest height change use case. In Sect. 2, we describe the study areas, data, and methods used for both topics. Section 3 is dedicated to the methods and results of TanDEM-X InSAR height validation for all study areas. In Sect. 4, we present the methods focussed on the forest height change analysis and corresponding validation results in one of the study areas suitable for this purpose. The results of the InSAR height validation and its use for canopy height change applications are discussed in Sect. 5.

2 Materials and Methods

2.1 Study Areas

Three areas were used for the validation of TanDEM-X DEMs. The areas represent temperate broadleaf forests in Germany and hemi-boreal forests in the transition zone between temperate broadleaf and boreal coniferous forests in Estonia (Fig. 1a). The study area “Hainich” is in a mountain range in central Germany with rolling terrain and some steeper slopes. The northern part of the area is managed and consists of coniferous stands, whereas the southern part is mainly covered by deciduous trees and belongs to the “Nationalpark Hainich”. The study area where all data overlap covered about 700 km². The study area “Eifel” is in the northern part of the low mountain range Eifel in West Germany and covers about 570 km². The area consists of a few steep slopes. Similar to Hainich, the major part of the area belongs to a national park (“Nationalpark Eifel”), where also mixed stands can be

found. The third study area “Risti” is in Northwest Estonia and represents a typical moraine landscape with flat-to-moderately undulating relief. Unlike the two other study areas, the forest is intensively managed and dominated by homogeneous single-species stands of uniform age. Numerous clearcutting activities can be observed in the study area. Therefore, it is of particular interest to assess the quality of height change retrieved from TanDEM-X in this study area. The spatial extent of this study area was 1500 km². Non-forest areas like grasslands and croplands as well as herbaceous wetlands have a small canopy height, whereas canopy heights within forests range mainly between 10 and 30 m. The forests in Hainich have the highest canopy heights amongst the three study areas followed by Eifel and Risti (Fig. 1b).

2.2 Data

2.2.1 TanDEM-X Data

This study is based on SAR data acquired by the TanDEM-X mission. We used operational datasets acquired for the generation of the global TanDEM-X DEM (Rizzoli et al. 2017), and the global TanDEM-X DEM 2020 (Wessel et al. 2022), focussing on the latter as of 2017 (Table 1). All data were acquired in StripMap mode with a spatial resolution of about 3 m and roughly 10–12 m independent posting for InSAR DEMs. The TanDEM-X data were acquired in HH (horizontal–horizontal) single polarisation. Two acquisitions for Risti from July 01, 2012 and July 28, 2018 and one acquisition for each of the study areas in Hainich and Eifel July 20, 2018 and May 09, 2018 were analysed (Table 1).

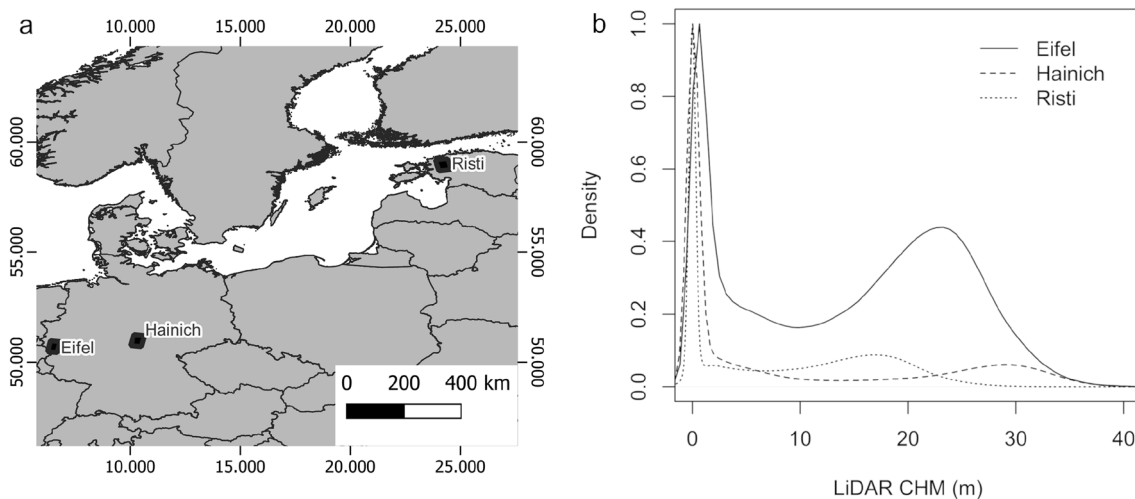


Fig. 1 Location of the three study areas (a) and relative density plot of their LiDAR canopy height models (b; CHM = DSM-DTM)

Table 1 Acquisition details of the TanDEM-X data and the LiDAR scans for the three test sites (HoA stands for Height of Ambiguity)

Area	Acquisition date (TanDEM-X)	HoA (m)	Look angle (°)	Orbit	Acquisition period(LiDAR)
Hainich, Germany	July 20, 2018	52.7	38.4	Descending	December 2016–March 2017
Eifel, Germany	May 09, 2018	56.5	46.3	Descending	February 2016–April 2016
Risti, Estonia (t0)	July 01, 2012	33.4	41.4	Ascending	April 25, 2012 and May 01, 2012
Risti, Estonia (t1)	July 28, 2018	54.9	36.2	Descending	May 28 and 29, 2018

2.2.2 Airborne LiDAR Data

The airborne LiDAR data for the German areas Eifel and Hainich were provided by the Federal States of North Rhine-Westphalia (Geobasis NRW 2022) and Thuringia, Germany (©GDI-Th) (Thüringer Landesamt für Bodenmanagement und Geoinformation (TLBG) 2022). The data accuracy is specified as ± 30 cm horizontally and ± 15 cm vertically. The data in Eifel were acquired from December 2016 to March 2017 and in Hainich from February 2016 to April 2016 (Table 1). The LiDAR data were classified into ground and non-ground points, which were further processed into DTM and DSM. The maximal height value within a grid cell was used to extract the surface height, as it was frequently used as reference height for the assessment of InSAR heights (Kugler et al. 2014; Schlund et al. 2019a). The official German geoid GCG2016 was applied to the data for the transformation from normal heights in DHHN2016 to ellipsoidal heights in WGS84.

For the Risti area, bi-temporal LiDAR acquisitions were available that matched very close the TanDEM-X acquisition dates. A DTM and a canopy height model (CHM) with a resolution of 10 m acquired with LiDAR between 25 April 2012 and 05 May 2012 were provided by the Estonian Land Board (2021). A second scan was acquired between May 28 and 29, 2018. The corresponding CHM data were available at 4 m resolution, which was also provided by the Estonian Land Board (2021). For the comparison with TanDEM-X DEMs, all elevation data given as orthometric heights in EH2000 height were transformed to WGS84 ellipsoidal heights with the geoid EST-GEOID2017 that was provided by Estonian Land Board (Ellmann et al. 2017). The LiDAR DEMs were projected and resampled into the exact grid of the TanDEM-X DEM data (0.4×0.6 arc seconds, longitude \times latitude) in geographic coordinates.

2.2.3 Copernicus Data

Copernicus High-Resolution Layers (HRL Forest), (<https://land.copernicus.eu/pan-european/high-resolution-layers/forests>) provide information with pan-European coverage, for the years 2012 at 20 m and 2018 at 10 m resolution (European Union 2022). They are generally

consistent with the TanDEM-X acquisitions and DEM resolutions. In this study, the Forest Type (FTY) layers of the respective years were used to distinguish between forest and non-forest areas. The Copernicus DEM (COP-DEM_GLO-90) (DOI: <https://doi.org/10.5270/ESA-c5d3d65>), which is derived from an edited version of the TanDEM-X DEM named WorldDEM™ based on acquisitions between 2010 and 2014, was used for the slope calculation where the slope itself was determined from the vicinity of 3 by 3 pixels.

2.3 TanDEM-X InSAR Height Retrieval

2.3.1 TanDEM-X DEM Processing

The InSAR DEMs of the TanDEM-X mission, the so-called RawDEMs (for acquisitions between 2010 and 2014) and Change RawDEMs (for acquisitions between 2017 and 2020), were explicitly utilised for this study. In general, (Change) RawDEMs are intermediate products and the output of the operational Integrated TanDEM-X Processor (ITP) of the German Aerospace Center (DLR). For the RawDEM and the Change RawDEM generation, the ITP processed the Coregistered Single look Slant range Complex (CoSSC) images to interferograms, which were further unwrapped and geocoded. For the Risti study area, the acquisition from 2012 was processed with the former, single-baseline phase unwrapping approach (Rossi et al. 2012). An individual height offset of 0.67 m for that acquisition was applied that was estimated within the operational TanDEM-X block adjustment over larger areas within the Mosaicking & Calibration Processor (MCP) (Gruber et al. 2012). The data from 2018 were processed with the so-called delta-phase unwrapping approach that calibrated the used InSAR data to TanDEM-X heights without the need for further height offset correction (Lachaise et al. 2020; Schweissshelm et al. 2020). The number and density of interferometric fringes was reduced by subtracting an edited version of the global TanDEM-X DEM from the acquired interferometric phase in the delta-phase unwrapping approach.

2.3.2 Penetration Depth Compensation

Despite its short wavelength, it can be assumed that the X-band penetrates to a certain extent into the canopy of the forests (Schlund et al. 2019a). This would mean that the penetration affects the accuracy of TanDEM-X InSAR heights over forests. Furthermore, varying penetration depths of the individual TanDEM-X acquisitions would result in pseudo-changes, and thus, inaccuracies in the InSAR height change estimation. Therefore, a penetration depth compensation for each InSAR data was applied. It was assumed that the phase information of the interferometric coherence was related to the penetration and that the coherence magnitude used to estimate the penetration depth had a unique relationship to its phase (Dall 2007; Schlund et al. 2019a). The respective volume coherence used in this model was calculated as the division of the estimated interferometric coherence and the signal-to-noise coherence, assuming that these were the main contributions (Martone et al. 2012; Rizzoli et al. 2022). This first-order approximation of the penetration depth was applied pixel-by-pixel to compensate for its effect on TanDEM-X InSAR heights.

3 Single-Date Analysis of TanDEM-X DEM 2020

The accuracy of InSAR heights processed for the TanDEM-X DEM 2020 collection is so far unexplored. It can be assumed that it provides both an indication of the quality of a single acquisition and a preview of the new TanDEM-X DEM 2020. Therefore, we first assessed the quality of these DEM data individually for each study area.

3.1 Methods for the Assessment of TanDEM-X InSAR Heights

The accuracy of the TanDEM-X InSAR heights was quantitatively assessed in comparison to the LiDAR DSM in the respective study areas. The root-mean-square-error (RMSE), mean error (ME), and coefficient of determination (R^2) were used to estimate the accuracy. For the visual comparison, the TanDEM-X heights were normalised with the LiDAR DTM to TanDEM-X interferometric phase centre heights above the terrain elevation, called TanDEM-X CHM in the following. Correspondingly, the LiDAR CHM was calculated by subtracting the LiDAR DTM from LiDAR DSM. The evaluation of the different elevation models was performed pixel-by-pixel.

The LiDAR CHMs were further stratified into a non-vegetation, low vegetation, and forest stratum to provide more information about the error structure of the TanDEM-X heights. Non-vegetation was defined as actual LiDAR

canopy height lower than 0.5 m. The low vegetation stratum was defined as actual canopy height above 0.5 m and below 5 m, whereas forest was defined as actual canopy height above 5 m.

In addition to the canopy height strata, the accuracy was assessed in two slope strata, namely above and below 10% of slope. The slope was calculated from the Copernicus DEM in 3 arc seconds. Also, elevation values over water bodies were masked out by the Copernicus water body mask which was derived from non-coherent InSAR elevation values. In contrast to the vegetation strata, the InSAR phase centre should optimally represent the surface height over bare soil areas, i.e., non-vegetation stratum. Therefore, the accuracy in non-vegetation with slopes below 10% excluding water bodies was assumed to provide best results due to the minimal effect of slope, vegetation, and water.

3.2 Results of TanDEM-X InSAR Height Validation

The 2D density plots of TanDEM-X CHM and LiDAR CHM suggested a general underestimation increasing with canopy height in all study areas (Fig. 2). Nevertheless, the deviation from the 1:1 line of TanDEM-X CHM versus LiDAR CHM was small at low canopy heights in all three study areas. After applying the penetration depth compensation, the TanDEM-X CHM was much closer to the 1:1 line for larger canopy heights, but resulted in an overestimation of small or none canopy heights (Fig. 2).

This was confirmed by the quantitative assessment, where the negative ME indicated a general underestimation of the the TanDEM-X InSAR heights in vegetation. In general, the highest errors in terms of ME and RMSE were observed in the forest stratum for the original heights. This was substantially improved by applying the penetration depth compensation (Table 2). The ME reduced from around -6 m for all three study areas to sub-metre range. Highest accuracies of the original TanDEM-X InSAR heights were generally achieved in the non-vegetation stratum. The RMSE and ME in the non-vegetation and low vegetation strata suggested that the penetration depth compensation resulted in over-compensation, with larger errors compared to the original InSAR heights in these strata (Table 2).

The assessment of slope effects in non-vegetated areas revealed that the RMSE of the original TanDEM-X InSAR heights was generally below 2 m when slopes were less than 10%. The RMSE increased on slopes above 10% compared to the flatter areas. This was the case for both height variants (i.e., without and with penetration depth compensation). The RMSE increase was highest in the Eifel study area, where areas with a slope above 10% comprised a larger proportion compared to other study areas (Table 3). In general, TanDEM-X InSAR heights achieved the highest accuracies in terms of RMSE, ME, and R^2 in areas without vegetation and with low slope.

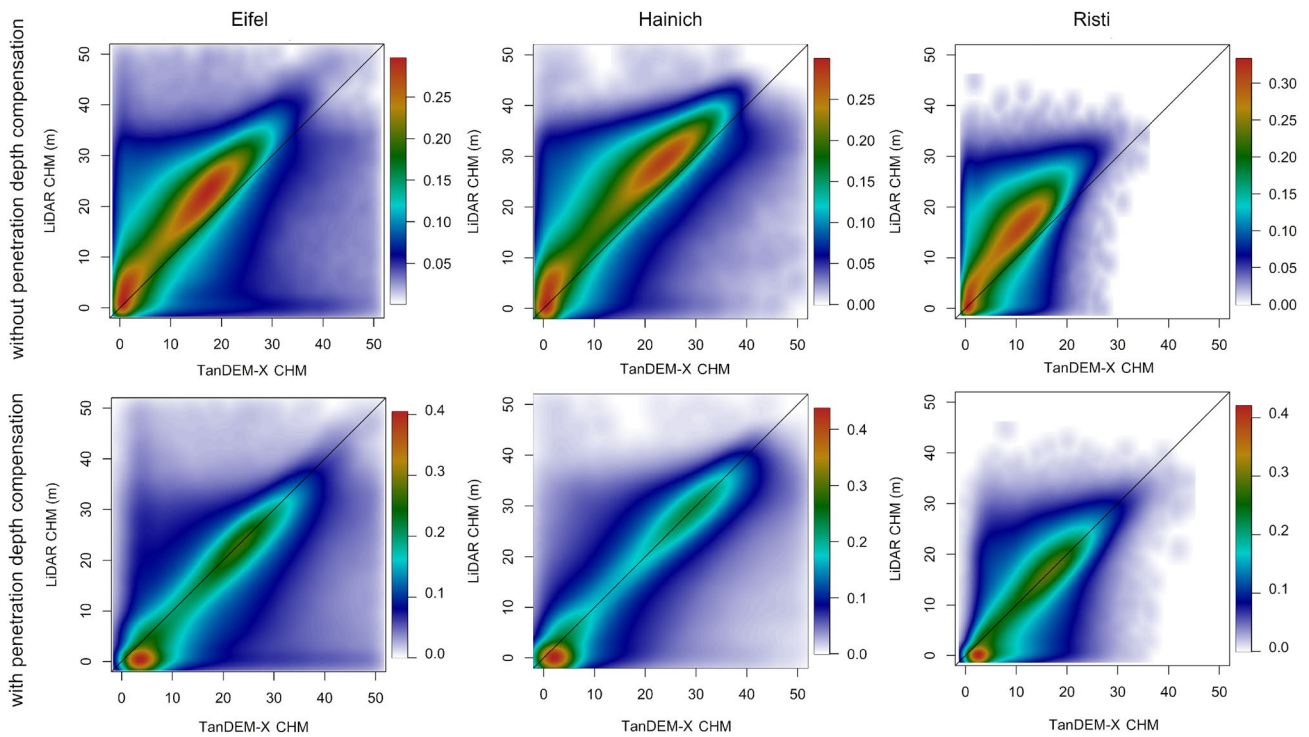


Fig. 2 2D density plots of LiDAR CHM and TanDEM-X CHM without penetration depth compensation (top) and with overall penetration depth compensation (bottom) in the Eifel (left), Hainich (centre), and Risti (right) study areas

Table 2 Accuracy assessment of TanDEM-X InSAR heights compared to LiDAR DSM in different canopy height strata in the three study areas

Area	Canopy height stratum	Coverage of stratum (%)	Original			Penetration depth compensation		
			RMSE (m)	ME (m)	R^2	RMSE (m)	ME (m)	R^2
Eifel	All	100	5.77	-3.85	0.99	4.66	2.08	0.99
	Vegetation (≥ 5 m)	57.0	7.25	-5.74	0.99	4.52	0.84	0.99
	Low vegetation (≥ 0.5 m & < 5 m)	18.1	3.30	-1.60	0.99	5.20	3.65	0.99
	Non-vegetation (< 0.5 m)	24.9	2.30	-1.17	0.99	4.56	3.79	0.99
Hainich	All	100	4.91	-3.30	0.99	3.35	1.12	0.99
	Vegetation (≥ 5 m)	39.4	7.40	-6.15	0.99	4.04	-0.32	0.99
	Low vegetation (≥ 0.5 m & < 5 m)	12.5	3.24	-2.31	0.99	3.43	1.74	0.99
	Non-vegetation (< 0.5 m)	48.0	1.57	-1.22	0.99	2.61	2.15	0.99
Risti	All	100	5.77	-4.07	0.92	3.72	0.70	0.93
	Vegetation (≥ 5 m)	65.6	6.99	-5.92	0.91	3.55	-0.54	0.92
	Low vegetation (≥ 0.5 m & < 5 m)	13.6	2.66	-0.91	0.96	4.57	3.05	0.92
	Non-vegetation (< 0.5 m)	20.9	1.26	-0.30	0.99	3.63	3.07	0.98

Table 3 Accuracy assessment of original TanDEM-X InSAR heights in the non-vegetation stratum (< 0.5 m) for different slope strata in the three study areas

Area	Slope	Coverage (%)	Original			Penetration depth compensation		
			RMSE (m)	ME (m)	R^2	RMSE (m)	ME (m)	R^2
Eifel	< 10%	90.9	1.88	- 1.15	0.99	4.30	3.78	0.99
	≥ 10%	9.1	4.25	- 0.83	0.99	6.88	4.70	0.99
Hainich	< 10%	95.1	1.54	- 1.35	0.99	4.30	3.80	0.99
	≥ 10%	4.9	1.94	1.21	0.99	4.18	3.55	0.99
Risti	< 10%	99.9	1.34	- 0.29	0.99	4.69	4.10	0.96
	≥ 10%	< 0.1	2.32	0.18	0.96	5.30	4.15	0.90

Therefore, these accuracies could be assumed to be the highest achievable accuracies in the respective study area.

4 Use Case: Forest Canopy Height Change Assessment

The accuracy assessment of the newly collected TanDEM-X acquisitions, which are the input data for the TanDEM-X DEM 2020, revealed a high accuracy for the individual DEMs. It can be anticipated that an important application of this additional coverage is the combination with accurate TanDEM-X DEMs acquired for the generation of the first global TanDEM-X DEM. This combination would provide high-resolution information about height changes in the last decade. Therefore, we studied the potential of the InSAR heights from the two global acquisitions to estimate changes in forest canopy height as a potential use case. For this analysis, we focussed on the study area Risti as the bi-temporal acquisition dates of TanDEM-X and LiDAR reference data fitted best with about two month difference for each. Furthermore, the Risti area is more dynamic in terms of canopy height changes due to observed clearcutting and forest regrowth compared to the other study areas with protected national parks.

4.1 Methods for the Assessment of Canopy Height Change Estimates

4.1.1 Selective Penetration Depth Compensation

The model to estimate the penetration depth was only valid in areas with high vegetation canopy height, i.e., negligible ground contribution to the signal (Dall 2007; Schlund et al. 2019a). This was confirmed by our results showing higher ME and RMSE values for the compensated heights compared to the original heights in the low and no vegetation stratum (see Sect. 3.2). A high accuracy over all canopy heights is generally desirable and particularly relevant when assessing canopy height changes, where land cover changes from forest to non-forest and vice versa. Therefore,

we added an additional compensation variant expecting an improved performance in the low and no vegetation stratum compared to the overall penetration depth compensation. For this variant, called “selective penetration depth compensation” in the following, the compensation of penetration depth was restricted to forest areas, whereas the original InSAR heights without penetration depth compensation were used in low and no vegetation. Note that the no and low vegetation stratum form the non-forest class. The non-forest class of the Copernicus High-Resolution Forest Type Layer (FTY) 2012 was used to mask TanDEM-X InSAR height values of 2012 to be excluded from penetration depth compensation. Similarly, FTY 2018 was used for masking TanDEM-X InSAR heights acquired in 2018. Consequently, the masked areas retained the original TanDEM-X heights, whereas the penetration depth compensation was applied to the areas classified as forest in the FTY layers. Note that FTY forest definition follows as far as possible Food and Agriculture Organization (FAO) forest definition (Copernicus Land Monitoring Service (CLMS) 2021; FAO 2018).

The focus on forest canopy height change required a more detailed look at the error of the non-forest class in case of forest removal as well as a more detailed analysis of the forest class and the effectiveness of the selective penetration depth compensation. To gain a better understanding of the error structure of the TanDEM-X InSAR heights in forest areas, the LiDAR CHM from 2012 was stratified into six height strata in 5 m intervals for the accuracy assessment. The accuracy of the original TanDEM-X InSAR heights from 2012 as well as 2018 and the corresponding penetration depth compensation variants were compared to the respective LiDAR DSMs.

Table 4 Change type classification based on LiDAR CHMs

Change type	Definition	Area (ha)
Forest loss	$CHM_{2012} \geq 5 \text{ m}$ $CHM_{2018} < 5 \text{ m}$	4171
Standing forest	$CHM_{2012} \geq 5 \text{ m}$ $CHM_{2018} \geq 5 \text{ m}$	49,351
Regrowth	$CHM_{2012} < 5 \text{ m}$ $CHM_{2018} \geq 5 \text{ m}$	1750

4.1.2 Change Type Classification

For assessing canopy height changes, the forest of the study area Risti, Estonia was classified based on height changes between the LiDAR CHM from 2012 and 2018. Three change types were distinguished: forest loss, regrowth, and standing forest changes (Table 4). The latter included smaller variations in mostly stable forested areas potentially induced by natural forest growth or forest management operations like thinning or selective harvesting. Note that the change types regrowth and forest loss were defined as stand replacing changes involving a change from forest to non-forest or vice versa in the time interval between 2012 and 2018. For this purpose, canopy heights of more than 5 m were defined as forest. It can be assumed that the dominant form of stand replacing forest loss in the Risti study area was clearcutting and seed tree harvesting.

4.1.3 Pixel-Wise Assessment of Canopy Height Changes

The pixel-wise height change $(\Delta H_{TDX})_{\text{pixel}}$ between 2012 and 2018 was defined as the difference of TanDEM-X heights of the new $(H_{TDX})_{2018}$ and TanDEM-X heights $(H_{TDX})_{2012}$ from the first global acquisitions

$$(\Delta H_{TDX})_{\text{pixel}} = (H_{TDX})_{2018} - (H_{TDX})_{2012}. \quad (1)$$

The temporal difference was calculated for all TanDEM-X InSAR height variants: (a) the original InSAR heights, (b) the InSAR heights with overall penetration depth compensation, and (c) the InSAR heights with selective penetration depth compensation. The pixel-wise height change

$(\Delta H_{\text{LiDAR}})_{\text{pixel}}$ of the reference LiDAR DSMs was computed in the same manner

$$(\Delta H_{\text{LiDAR}})_{\text{pixel}} = (H_{\text{LiDAR}})_{2018} - (H_{\text{LiDAR}})_{2012}. \quad (2)$$

Consequently, height increase or forest growth over time resulted in positive values and height decrease or forest loss was reflected by negative values. The TanDEM-X canopy height change error $(\Delta H_{\text{Error}})_{\text{pixel}}$ was defined as the difference between TanDEM-X $(\Delta H_{\text{TDX}})_{\text{pixel}}$ and LiDAR height change $(\Delta H_{\text{LiDAR}})_{\text{pixel}}$

$$(\Delta H_{\text{Error}})_{\text{pixel}} = (\Delta H_{\text{TDX}})_{\text{pixel}} - (\Delta H_{\text{LiDAR}})_{\text{pixel}}. \quad (3)$$

The quality measures RMSE, ME, and R^2 were computed to assess the accuracy of TanDEM-X canopy height changes. The accuracy analysis was performed for all pixels and separately for each change type (regrowth, standing forest, and forest loss) to discriminate between substantial positive and negative as well as low magnitude changes (see Sect. 4.1.2).

4.1.4 Stand-Wise Assessment of Canopy Height Changes

Due to considerable errors in InSAR heights in forests (Table 2), the height estimates need to be further aggregated to improve the estimation of small variations. For this purpose, we intended to use the spatial unit of forest stands, which is commonly used in forestry. Stand borders were approximated from the LiDAR data to retrieve homogeneous forest areas. The conducted change type classification provided the areas of forest loss and regrowth stands (see Sect. 4.1.2). However, most of the area was classified as

Table 5 Accuracy assessment of TanDEM-X InSAR heights from 2012 and 2018 with different levels of penetration depth compensation in different canopy height strata in the Risti study area

Year	Canopy height stratum (m)	Coverage of stratum (%)	Penetration depth compensation								
			None			Overall			Selective		
			RMSE	ME	R^2	RMSE	ME	R^2	RMSE	ME	R^2
2012	All	100	4.18	-2.28	0.79	3.31	1.21	0.84	3.58	0.24	0.78
	< 5	28.0	2.08	-0.54	0.97	3.18	2.03	0.96	2.70	0.39	0.95
	≥ 5–10	15.5	4.02	-2.85	0.94	3.23	0.97	0.93	3.65	0.22	0.91
	≥ 10–15	25.0	5.00	-3.93	0.93	3.05	0.47	0.93	3.40	0.23	0.91
	≥ 15–20	25.3	5.85	-4.48	0.89	3.57	0.32	0.91	3.77	0.23	0.90
	≥ 20–25	5.8	7.85	-5.37	0.77	5.53	-0.08	0.79	5.69	-0.16	0.78
	≥ 25	0.4	11.94	-7.21	0.50	9.54	-1.75	0.51	9.69	-1.84	0.51
2018	All	100	5.25	-3.26	0.79	3.89	1.26	0.81	3.72	-0.49	0.80
	< 5	34.5	1.93	-0.54	0.98	4.02	3.06	0.96	2.99	0.28	0.95
	≥ 5–10	13.4	4.14	-3.22	0.95	3.47	1.27	0.93	4.03	0.39	0.89
	≥ 10–15	19.2	5.66	-4.99	0.95	2.87	0.07	0.94	3.48	-0.27	0.91
	≥ 15–20	24.5	7.18	-6.49	0.93	3.14	-0.91	0.93	3.57	-1.06	0.91
	≥ 20–25	10.6	9.59	-8.70	0.88	4.57	-2.38	0.89	5.00	-2.53	0.86
	≥ 25	1.9	12.92	-11.69	0.77	7.07	-4.49	0.78	7.68	-4.72	0.74

standing forest with small canopy height changes (Table 4). Consequently, a further subdivision into forest stands with homogenous heights was necessary to support a stand-wise assessment. To create homogenous areas of standing forests, the initial heights of LiDAR CHM from 2012 were stratified into the same six height classes of 5 m intervals listed in Table 5. Finally, a minimum mapping unit of 0.5 ha was applied to remove very small stand polygons. This resulted in 683 stands for the regrowth change type with an average size of 2.56 ha and standard deviation of 2.27 ha. For the forest loss change type, 2624 stands with an average size of 1.59 ha and standard deviation of 1.55 ha were available. As mentioned, the largest part of the area was covered by standing forest with 28,482 stands with an average size of 1.75 ha and a standard deviation of 1.55 ha. The mean height change estimates from LiDAR and TanDEM-X were extracted for the stand polygons. The stand-wise forest height change accuracy ($\Delta H_{\text{Error}}_{\text{Stand}}$) was assessed using the difference in mean delta heights between TanDEM-X and LiDAR for each forest stand, similar to the pixel-wise assessment.

4.2 Results of Canopy Height Change Validation

4.2.1 Results of the Different Penetration Depth Compensations

In line with the single-date analysis, the original InSAR heights achieved the highest accuracy in the non-forest stratum for both acquisition dates. The accuracy generally decreased with increasing canopy height stratum. The overall penetration depth compensated InSAR heights showed improved results for all forest strata with highest accuracies in the 10–15 m stratum. Again, the non-forest stratum resulted in lower accuracies compared to the original heights indicating an overcompensation of the penetration depth in those areas. In contrast, the selective penetration depth compensation achieved highest accuracy in the non-forest stratum (CHM < 5 m) with RMSE of 2.70 m in 2012 and

2.99 m in 2018. The overall as well as the selective penetration depth compensation achieved similar accuracies in the vegetation strata between 5 and 25 m with an RMSE ranging from 2.87 to 5.69 m and thus showed a considerable improvement compared to original TanDEM-X InSAR heights (Table 5).

4.2.2 Results of Pixel-Wise Change Validation

Table 6 presents the results of the pixel-wise as well as stand-wise accuracy assessment. The pixel-wise results obtained by the selective penetration bias compensation resulted in height change ME values of -1.12 m for forest loss, -0.80 m for standing forest and -0.56 m for regrowth. This underestimation of the mean height change (i.e., as difference between TanDEM-X height change and LiDAR height change) was relatively small compared to the RMSE values between 7.31 m for forest loss, 4.56 m for standing forest and 5.01 m for regrowth. The 2D density plots of the selectively compensated TanDEM-X height differences compared to the LiDAR differences confirmed this observation (Fig. 3). As it can be observed in Table 6, the RMSE values of the overall and the three change classes forest loss, regrowth, and standing forest did not differ substantially amongst the three TanDEM-X height variants. In contrast to RMSE, the R^2 improved for the selective penetration depth result. The most evident difference between the three different penetration depth compensation methods was the decrease in ME. The ME for the pixel-wise change estimates was highest for the original TanDEM-X InSAR heights and lowest for heights with selective penetration depth compensation (Table 6).

4.2.3 Results of Stand-Level Change Validation

The assessment of canopy height changes on stand level resulted in substantial improvements compared to the assessment on pixel level. The largest improvement was achieved

Table 6 Pixel- and stand-wise accuracy of TanDEM-X height changes between 2012 and 2018 in forests with different levels of penetration depth compensation calculated as overall accuracy and by change class in the Risti study area

Level	Change Type	Penetration depth compensation								
		None			Overall			Selective		
		RMSE	ME	R^2	RMSE	ME	R^2	RMSE	ME	R^2
Pixel	Overall	4.17	-0.93	0.29	4.01	0.09	0.33	4.06	-0.53	0.38
	Clearcut	7.61	2.78	0.11	7.45	2.49	0.14	7.31	-1.12	0.15
	Standing forest	4.90	-1.81	0.01	4.47	-0.79	0.02	4.56	-0.80	0.03
	Regrowth	5.31	-2.42	0.03	4.96	-1.54	0.04	5.04	-0.56	0.03
Stand	Overall	2.84	-1.48	0.74	2.16	-0.55	0.81	2.14	-0.83	0.84
	Clearcut	4.12	2.90	0.47	3.88	2.62	0.51	3.28	-0.85	0.51
	Standing forest	2.69	-1.86	0.12	1.93	-0.82	0.18	2.01	-0.83	0.19
	Regrowth	2.81	-2.31	0.06	2.19	-1.43	0.06	1.91	-0.46	0.06

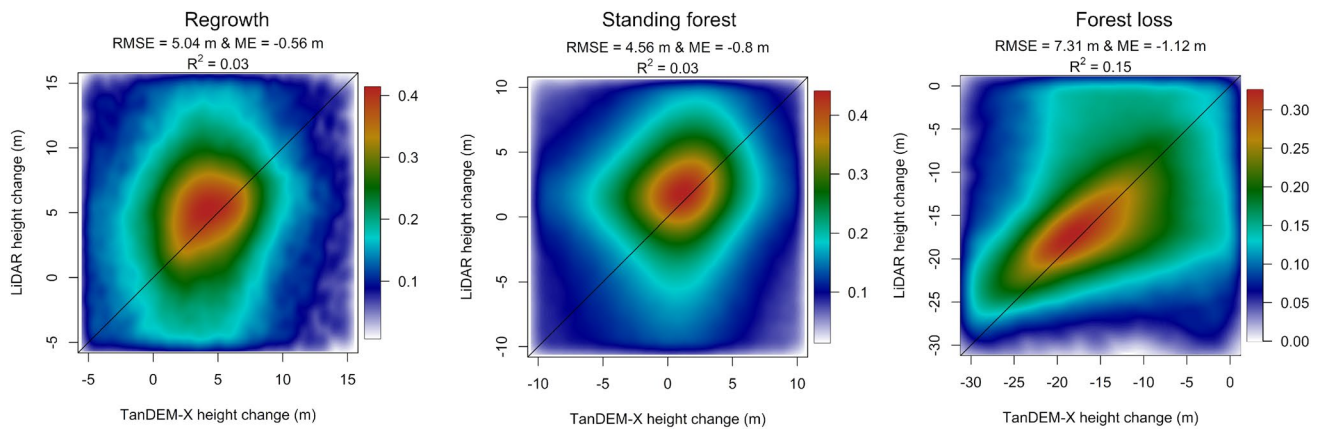


Fig. 3 2D density plots of pixel-wise LiDAR and TanDEM-X height changes with selective penetration depth compensation differentiated in forest height change classes, Risti (left = regrowth, centre = standing forest changes, and right = forest loss)

in the forest loss class with a decrease in RMSE from 7.31 to 3.28 m for the selective penetration compensation. The RMSE also improved for standing forest and regrowth from 4.56 and 5.04 m to 2.01 and 1.91 m. The highest improvement for the ME was achieved with the selective penetration bias compensation compared to without or overall compensation methods. The ME values improved from -1.86 and -2.31 m without compensation to -0.83 m and -0.46 m with selective penetration compensation in the standing forest and regrowth class. The R^2 of the overall accuracy analysis increased substantially from 0.74 for the original InSAR heights to 0.81 for overall, and to 0.84 for the selectively compensated heights (Table 6).

The effect of the penetration depth could be observed by deviations from the 1:1 line comparing TanDEM-X to LiDAR height change on stand level (Fig. 4). Original TanDEM-X InSAR heights generally indicated an underestimation of height changes between 0 and 5 m (Fig. 4 left), which was improved by the overall as well as the selective

penetration bias compensation resulting in values closer to the 1:1 line (Fig. 4 centre and right). Larger negative changes of -20 to -10 m were substantially improved by the selective penetration depth compensation.

The 2D density plot of TanDEM-X and LiDAR change at stand-level confirmed the observations on pixel-level that a slight underestimation of height change in the forest loss stands compared to LiDAR were indicated by TanDEM-X. This was improved with the selective penetration compensation (Figs. 4 and 5). Furthermore, the different clusters in the standing forest class suggested a high heterogeneity of changes in those stands (Fig. 5). These details were not visible in the pixel-wise 2D density plot (Fig. 3).

Beyond the accuracy measures, the spatial distribution of the TanDEM-X height change variant with selective penetration depth compensation was compared to the LiDAR height changes (Fig. 6). The visual comparison of stand height changes across the study area revealed similar spatial patterns for TanDEM-X and LiDAR. In particular,

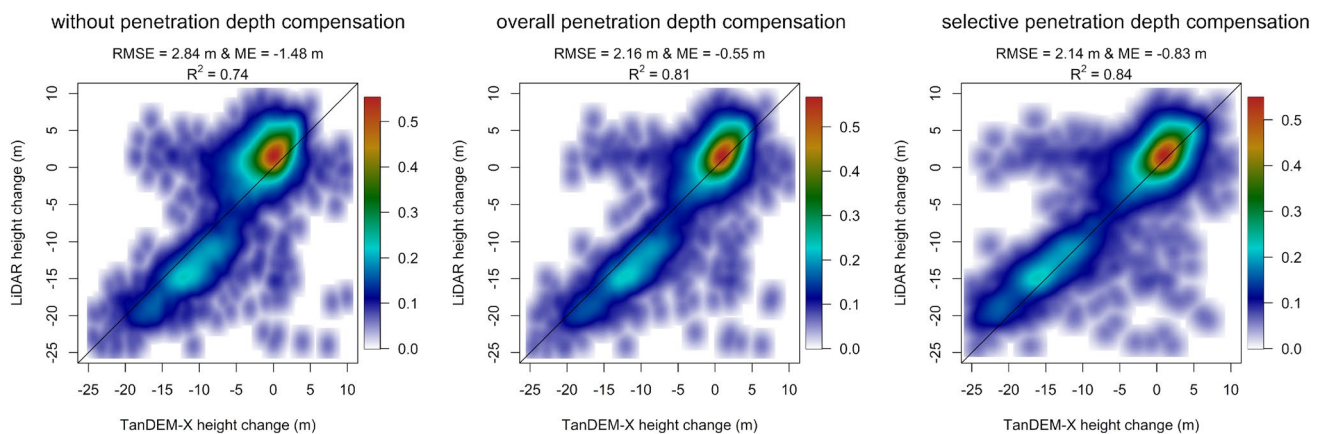


Fig. 4 2D density plots of stand-wise LiDAR and TanDEM-X height changes without penetration depth compensation (left), with overall penetration depth compensation (centre) and selective penetration depth compensation (right) for all forest stands in Risti

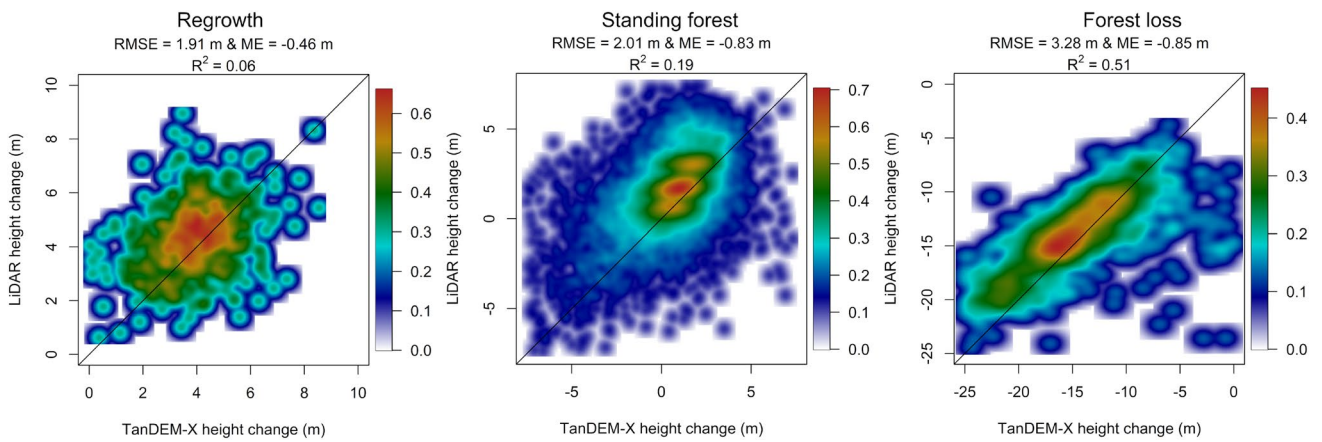


Fig. 5 2D density plots of stand-wise LiDAR and TanDEM-X height changes with selective penetration depth compensation differentiated in forest height change classes, Risti (left = regrowth, centre = standing forest changes, and right = forest loss)

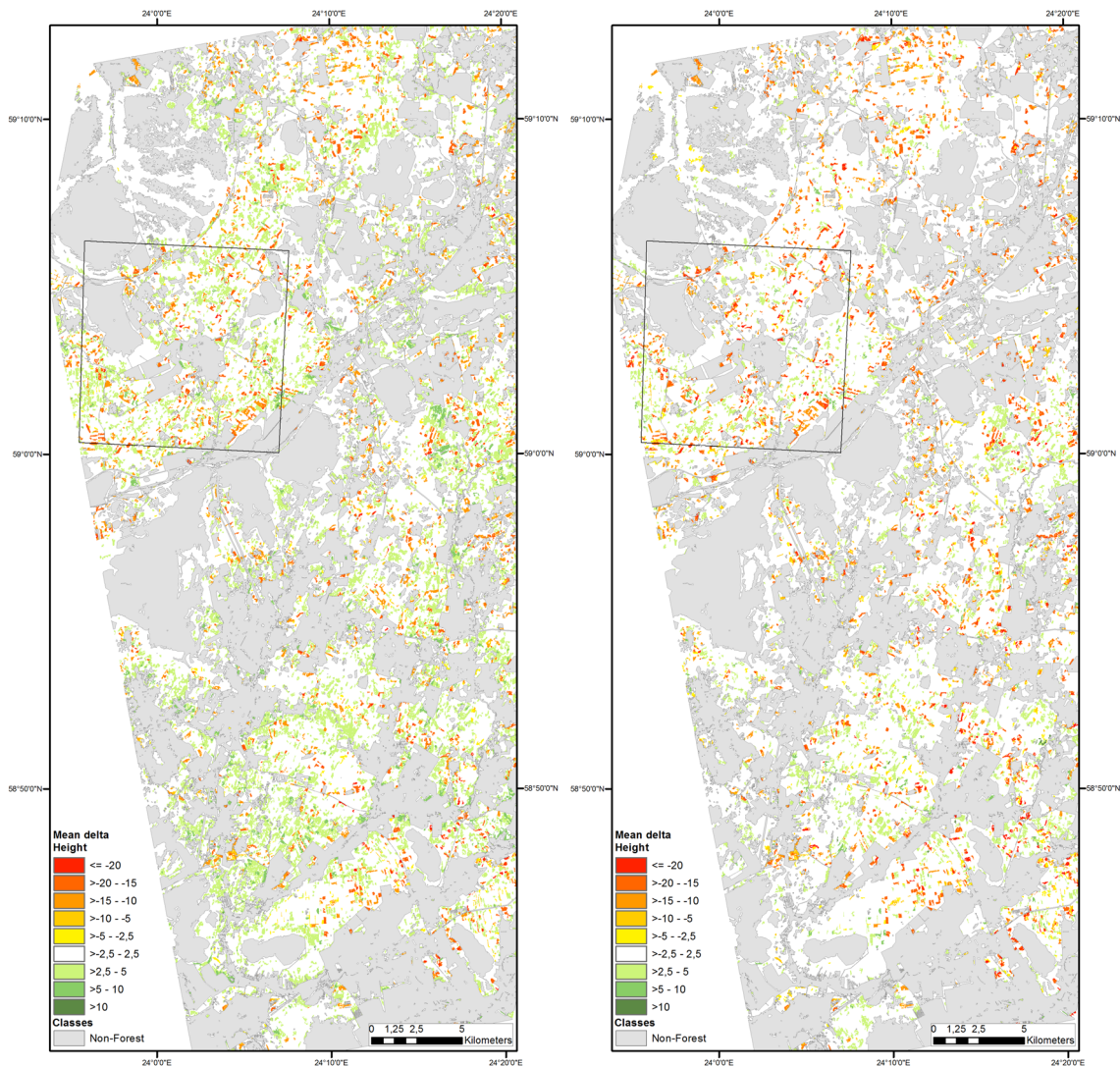


Fig. 6 Overview of stand-wise LiDAR height changes (left) and TanDEM-X height changes with selective penetration depth compensation (right)

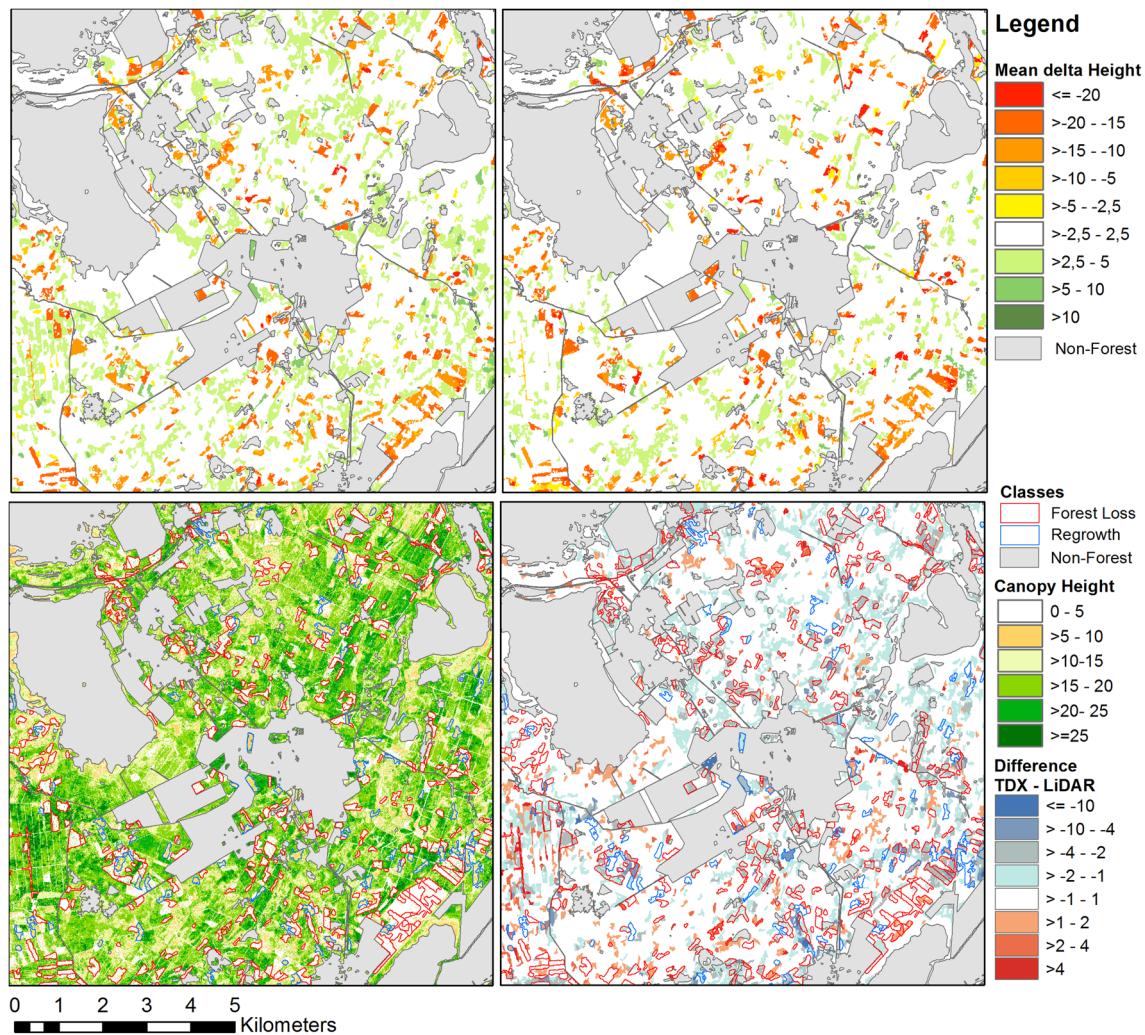


Fig. 7 Zoom-in of stand-wise height changes from LiDAR (top left) and TanDEM-X (top right), the pixel-wise canopy height from LiDAR reference of 2018 (bottom left), and difference of TanDEM-X

and LiDAR height changes (bottom right). Regrowth, forest loss, and non-forest stand polygons as overlay

the height changes in the forest loss class indicated by negative values corresponded well in the TanDEM-X and LiDAR maps. However, more forest growth areas in the range of 2.5–5 m were represented in the LiDAR compared to the TanDEM-X changes (Fig. 6).

The zoomed area confirmed that substantial changes classified as regrowth and forest loss (delineated by blue and red outlines, see also Sect. 4.1.2) were well captured as regions of growth (positive values above 2.5 m) and forest loss (negative values below – 10 m), respectively (Fig. 7). The difference of LiDAR and TanDEM-X changes suggested that regrowth areas differed less than 1 m in many stands (blue outline). In contrast, natural forest growth in the standing forest class (no outline) was often underestimated indicated in light blue (negative differences of – 1 to – 2 m, Fig. 7 bottom right).

5 Discussion

5.1 Assessment of TanDEM-X DEM 2020 Data

We evaluated TanDEM-X InSAR heights processed in the frame of the new TanDEM-X DEM 2020 with special focus on InSAR heights over forests. We assessed the InSAR height accuracy of individual acquisitions of the newly acquired and processed TanDEM-X DEM 2020 data using LiDAR as a reference data source for the accuracy analysis. It was assumed that vertical and horizontal accuracy of airborne LiDAR DEMs was substantially higher than that of TanDEM-X DEMs. Therefore, it can be considered as a suitable reference. Another important prerequisite for the investigation was

the temporal correspondence of the TanDEM-X acquisitions and LiDAR reference data. Here, the maximum difference between acquisition dates was about 2 years in Eifel and Hainich. However, both areas are mostly covered by national parks, so that it is expected that substantial temporal differences, e.g., caused by clearcut harvesting between the acquisitions, were minimal.

The TanDEM-X InSAR heights of the 2020 collection generally resulted in ME values between -3.3 and -4.1 m and RMSE values between 4.91 and 5.77 m for all heights. The highest inaccuracies could be attributed to the forest stratum (canopy height > 5 m). In this stratum, we found an underestimation (negative ME) of heights between 5.74 and 6.15 m in the three temperate and boreal study areas. These biases are in line with findings of previous studies where a systematic underestimation of forest canopy height was attributed to the signal penetration (Perko et al. 2011; Kugler et al. 2015; Schlund et al. 2019a). A higher penetration of up to 12 m was found in boreal and temperate forests in TanDEM-X data acquired in winter (Kugler et al. 2014). To overcome this deficiency, a model-based approach to compensate this height bias has been proposed, that achieved considerable improvements in the determination of forest canopy heights in temperate and tropical latitudes (Schlund et al. 2019a, 2021). The potential to compensate for the penetration was confirmed for all TanDEM-X InSAR heights that were evaluated in this study. However, the assessment of the penetration compensation was so far focussed only on forests (Schlund et al. 2019a, 2021; Wang et al. 2021). We found that the penetration depth compensation decreased the accuracy considerably for non-vegetated areas, but also for low vegetation with canopy heights below 5 m. It could be assumed that this is based on the fact that some of the model assumptions, such as infinite canopy height, were not valid and the signal had a considerable ground contribution (Dall 2007; Schlund et al. 2019a). This resulted in a substantial overcompensation of the penetration depth in the non-forest strata. Overall, the lowest RMSE of 1.26 m and smallest bias of 0.30 m was found in the non-vegetation stratum in Risti. It is a well-known fact that the accuracy also depends on the terrain slope and thus local incidence angle (Wessel et al. 2018; Sadeghi et al. 2016; Gdulová et al. 2021). The RSME over the non-vegetated stratum increased for slopes above 10% by 0.4 m to 2.4 m depending on the study area. Hojo et al. (2020) also suggested that canopy height models retrieved from TanDEM-X InSAR achieved highest performance at small slopes and suggested that slope is one of the most influential factors on the performance in a subsequent AGB estimation.

In general, the quality of TanDEM-X DEM 2020 indicated a high potential to estimate the absolute height of forest canopy surfaces with high accuracy. It can be used to calculate the forest canopy height (CHM) by subtracting

the terrain height (DTM), preferably measured by LiDAR. These findings are consistent with other studies analysing TanDEM-X InSAR heights for canopy height estimation (Sadeghi et al. 2016; Ullah et al. 2020; Hojo et al. 2020). In addition to subtracting a DTM from TanDEM-X InSAR heights for canopy height estimation, several studies estimated the canopy height using coherence-based inversion models with TanDEM-X with and without the support from DTMs (Kugler et al. 2014; Olesk et al. 2016; Schlund et al. 2019b; Gomez et al. 2021). For instance, canopy height estimations supported by a DTM achieved RMSE values of 1.58 m in a boreal forest and 3.3 m in temperate forest (Kugler et al. 2014). These approaches are generally limited to areas where a highly accurate DTM is available. However, in Europe, LiDAR-derived DTMs are widely available today (European Commission and Joint Research Centre et al. 2021), allowing a potential application of such information to estimate CHMs based on TanDEM-X DEM 2020 acquisitions at large scale. The LiDAR-based DTM may even be outdated, assuming that terrain height remains relatively stable over time.

5.2 Canopy Height Change Application

The quantification of canopy height changes can assist forest monitoring as well as carbon accounting. Therefore, TanDEM-X InSAR height changes were assessed to support the quantification of canopy height changes. It can be argued that the two global acquisitions of TanDEM-X from 2010 to 2014 and from 2017 to 2020 are an unprecedented data source to estimate canopy height changes on large to even global scale. For the change assessment, the study area with most consistent acquisition dates of the bi-temporal LiDAR reference data and TanDEM-X acquisitions was selected. For the other investigated sites, we expected that the temporal disagreement between reference and TanDEM-X data would lead to many uncertainties in the change assessment, as it was observed for example in the study by Gdulová et al. (2021).

The forest height change assessment demonstrated that if the compensation of signal penetration depth is only applied to forest areas the height bias of the contributing DEMs substantially reduced. In addition, the underestimation of loss and gain found in the change results of the original TanDEM-X InSAR heights decreased by applying the compensation. The two individual TanDEM-X datasets have been acquired in the same season in our study. However, Schlund et al. (2019a) demonstrated that also acquisitions from different seasons with differing dielectric properties were comparable after penetration depth compensation. To benefit from the high accuracies of the original InSAR height over non-vegetated surfaces and compensated heights in forested surfaces, the compensation approach was selectively applied

to forest areas using a forest map provided by the Copernicus Land Monitoring Service (European Union 2022). It is worth noting that the accuracy of the forest map propagates to the selective penetration compensation and height estimation, potentially decreasing their accuracy in cases of forest omissions. However, it can be anticipated that many applications require high accuracy of the InSAR in forests as well as non-forested areas. For instance, bare ground where clearcutting has taken place or regrowth on bare land is of high relevance when monitoring canopy height.

The change results at pixel resolution (12 m) provide a spatially detailed overview of changes induced by substantial forest loss and gain with low overall bias. Therefore, pixel-wise height change detection can provide an input to accurate deforestation, disturbance, and growth extent mapping by simple height change thresholding (Solberg et al. 2013; Tanase et al. 2015; Tian et al. 2017). For example, Tian et al. (2017) achieved a Kappa value of 0.7 for storm damage detection using TanDEM-X DEMs compared to WorldView DEMs with a kappa value of 0.78. Nevertheless, the pixel-level estimation bears high uncertainties for loss and growth in the quantification of canopy height changes. A pixel-wise comparison at the scale of tree crowns is particularly impacted by differing viewing properties when compared to LiDAR. This is also the case for a change assessment using bi-temporal TanDEM-X acquisitions, where tree crowns identified at each step in time have to be matched with each other. Here, the change of orbit direction between ascending at the first and descending at the second TanDEM-X DEM acquisition campaign (for the northern hemisphere) can potentially introduce an additional error source. It was assumed that these effects should decrease when estimates are derived over forest stands. In general, random noise and other potential error sources were reduced when aggregating at stand level.

Overall, the stand-wise change assessment resulted in a considerable improvement of R^2 from 0.38 on pixel to 0.84 on stand level and a decrease of RMSE from 4.06 to 2.16 m. A minimum polygon size of 0.5 ha was chosen as a trade-off between spatial detail and estimation error. Further, the FAO (2018) defines forests with a minimum area criterion of 0.5 ha. The achieved accuracies for forest loss stands (RMSE = 3.3 m), regrowth (RMSE = 1.91 m), and the low bias expressed as ME ranging between 0.46 and 0.85 m indicate the potential of the stand-wise height change for biomass change estimation. Solberg et al. (2014) stressed the fact that the use of surface models for carbon monitoring is very sensitive to height bias, since a small bias in height changes over large areas translates in considerable bias in AGB change. Despite the low RMSE of 2.01 m for changes in standing forests, the stand-wise 2D density plot suggests that further subdivisions by thinning, selective logging, and mainly natural forest growth might be distinguishable (Fig. 4). However,

due to their magnitude of change, it was considered to be too small and thus was summarised in one class. Nevertheless, the magnitude of disturbances caused by bark beetle in the Bohemian Forest seems to cause changes substantial enough to be detected by TanDEM-X height change analysis, even using lower quality SRTM as pre-event DEM (Gdulová et al. 2021). Regarding error propagation, the forest loss and growth estimation are mainly driven by the accuracies of the stratum of each input DEM. Considering the high accuracies for bare ground, it can be assumed that the accuracy depends mainly on the stand height and structure before disturbance or cutting. Compared to backscatter-based approaches, which normally suffer from saturation effects (Araza et al. 2022), larger canopy heights above 25 m still indicated a high correlation between TanDEM-X and LiDAR height changes with R^2 between 0.51 and 0.74 despite increased RMSE and ME.

6 Conclusion

In this study, we evaluated the potential exploitation of the TanDEM-X DEM archive for large-scale three-dimensional forest monitoring with special focus on TanDEM-X DEM 2020 acquisitions and processing.

The single-date analysis provided information on the error structure of the TanDEM-X InSAR heights. A penetration depth compensation approach was applied to reduce the underestimation of TanDEM-X heights typically found in forests. The effectiveness of this height bias compensation when stratified into non-vegetation, low vegetation, and forest was evaluated. Major findings were that both the bias and RMSE increased with vegetation height at the original TanDEM-X heights. The bias compensation was only effective for forests but overcompensated non-forest heights. The resulting selective compensation of penetration depth was an attempt to mitigate overcompensation of penetration depth in non-forest areas whilst achieving adequate compensation in forest areas. This approach demonstrated a decrease of the bias and RMSE over all heights. The case study over the managed forests in Risti, Estonia demonstrated that forest canopy height changes can be retrieved with low overall bias for 12 m pixel spacing over the whole range of changes. However, it was found that the quantitative change information was not very precise. At stand level with a minimum stand size of 0.5 ha, a decrease of RMSE of around 50% was achieved compared to pixel level. The study suggested that stand replacing changes such as clearcutting and regeneration with bare ground at one point in time can be quantified with low ME and RMSE. Future studies could confirm the high potential of TanDEM-X DEM 2020 and derived composited products for estimating canopy height and change in other areas. In comparison to backscatter or

reflectance-based estimation of carbon stock change proxies, saturation effects were not observed for TanDEM-X InSAR heights. Thus, the study demonstrated the effectiveness of the proposed approach for the measurement of actual forest canopy height in temperate and boreal areas and retrospective forest canopy change analysis over the last decade. Future bi-static or even multi-static InSAR missions could expand the potential of the TanDEM-X mission by enabling both regular consistent coverage and on demand tasking. This would allow canopy height monitoring with regular revisits and near-real time quantification of damages caused by natural or human disturbances.

Acknowledgements We would like to thank Carolin Walper for processing the LiDAR DEMs at Eifel and Sabine Baumann for supporting in the TanDEM-X DEM processing. The TanDEM-X data were provided by DLR under the TanDEM-X CoSSC science proposal XTI_VEGE7394. We acknowledge the use of the Copernicus Land Monitoring Service data, which were produced with funding by the European Union. EO data provided under COPERNICUS by the European Union and ESA. We acknowledge the Estonian Land Board for providing the LiDAR DEMs and licence to use the Estonian Geoid Model EST-GEOID 2017 for the Risti area. Geobasis NRW and Thüringer Landesamt für Bodenmanagement und Geoinformation (TLBG) are acknowledged to provide the LiDAR data for the Eifel and Hainich study areas.

Funding The study was supported in the frame of the IKEBANA project funded by the German Ministry for Economic Affairs and Energy (BMWi) (FKZ 50 EE 1808).

Data availability TanDEM-X CoSSC and DEM data can generally be requested and accessed at the Science Service System and EOWEB GeoPortal of the German Aerospace Center (<https://tandemx-science.dlr.de/>, <https://eoweb.dlr.de/egp/>). The LiDAR data of Hainich can be accessed at <https://www.geoportal-th.de/dede/Downloadbereiche/Download-Offene-Geodaten-Thüringen/Download-Höhendaten>, the LiDAR data of Eifel can be accessed at https://www.opengeodata.nrw.de/produkte/geobasis/hm/3dm_1_las/3dm_1_las/ and the LiDAR data of Risti can be accessed at <https://geoportaal.maaamet.ee/eng/Maps-and-Data/Elevation-data/Download-Elevation-Data-p664.html>. The Copernicus data used for this study can be accessed at <https://land.copernicus.eu/>.

Declarations

Conflict of interest The authors declare that they have no known competing financial interests or personal relationships that could have appeared to influence the work reported in this paper.

Open Access This article is licensed under a Creative Commons Attribution 4.0 International License, which permits use, sharing, adaptation, distribution and reproduction in any medium or format, as long as you give appropriate credit to the original author(s) and the source, provide a link to the Creative Commons licence, and indicate if changes were made. The images or other third party material in this article are included in the article's Creative Commons licence, unless indicated otherwise in a credit line to the material. If material is not included in the article's Creative Commons licence and your intended use is not permitted by statutory regulation or exceeds the permitted use, you will need to obtain permission directly from the copyright holder. To view a copy of this licence, visit <http://creativecommons.org/licenses/by/4.0/>.

References

- Abdullahi S, Kugler F, Pretzsch H (2016) Prediction of stem volume in complex temperate forest stands using TanDEM-X SAR data. *Remote Sens Environ* 174:197–211. <https://doi.org/10.1016/j.rse.2015.12.012>, <http://www.sciencedirect.com/science/article/pii/S0034425715302339>
- Araza A, de Bruin S, Herold M, Quegan S, Labriere N, Rodriguez-Veiga P, Avitabile V, Santoro M, Mitchard ET, Ryan CM, Phillips OL, Willcock S, Verbeeck H, Carreiras J, Hein L, Schelhaas MJ, Pacheco-Pascagaza AM, da Conceição Bispo P, Laurin GV, Vieilledent G, Slik F, Wijaya A, Lewis SL, Morel A, Liang J, Sukhdeo H, Schepaschenko D, Cavlovic J, GilanH, Lucas R (2022) A comprehensive framework for assessing the accuracy and uncertainty of global above-ground biomass maps. *Remote Sens Environ* 272:112917. <https://doi.org/10.1016/j.rse.2022.112917>, <https://www.sciencedirect.com/science/article/pii/S0034425722000311>
- Atkins JW, Walter JA, Stovall AEL, Fahey RT, Gough CM (2021) Power law scaling relationships link canopy structural complexity and height across forest types. *Funct Ecol* 36(3):713–726 <https://doi.org/10.1111/1365-2435.13983>, <https://besjournals.onlinelibrary.wiley.com/doi/abs/10.1111/1365-2435.13983>
- Coops NC, Tompalski P, Goodbody TR, Queinnec M, Luther JE, Bolton DK, White JC, Wulder MA, van Lier OR, Hermosilla T (2021) Modelling lidar-derived estimates of forest attributes over space and time: a review of approaches and future trends. *Remote Sens Environ* 260:112477. <https://doi.org/10.1016/j.rse.2021.112477>, <https://www.sciencedirect.com/science/article/pii/S0034425721001954>
- Copernicus Land Monitoring Service (CLMS) (2021) Copernicus Land Monitoring Service. High Resolution land cover characteristics. Tree-cover/forest and change 2015–2018. User Manual. European Environment Agency (EEA), European Union., Kongens Nytorv 6 - 1050 Copenhagen K. - Denmark, 1.2 edn, <https://land.copernicus.eu/user-corner/technical-library/forest-2018-user-manual.pdf>
- Dall J (2007) InSAR elevation bias caused by penetration into uniform volumes. *IEEE Trans Geosci Remote Sens* 45(7):2319–2324. <https://doi.org/10.1109/TGRS.2007.896613>
- Ellmann A, Märdla S, Oja T (2017) Estonian Geoid Model EST-GEOID 2017. Tech. rep., University of Technology, Tallinn
- Estonian Land Board (2021) Elevation data, Land Board 2012–2018. <https://geoportaal.maaamet.ee/eng/Maps-and-Data/Elevation-data/Download-Elevation-Data-p664.html>. Accessed 06 Aug 2021
- European Commission and Joint Research Centre, Florio P, Kakoulaki G, Martinez A (2021) Non-commercial Light Detection and Ranging (LiDAR) data in Europe. Publications Office. <https://doi.org/10.2760/212427>
- European Union (2022) Copernicus land monitoring service 2018, european environment agency (eea). <https://land.copernicus.eu>. Accessed 09 Feb 2022
- FAO (2018) Global Forest Resources Assessment 2020. Terms and Definitions. In: FRA 2020. FAO, Rome
- Feng G, Zhang J, Girardello M, Pellissier V, Svenning JC (2020) Forest canopy height co-determines taxonomic and functional richness, but not functional dispersion of mammals and birds globally. *Glob Ecol Biogeogr* 29(8):1350–1359. <https://doi.org/10.1111/geb.13110>
- Forzieri G, Girardello M, Ceccherini G, Spinoni J, Feyen L, Hartmann H, Beck PSA, Camps-Valls G, Chirici G, Mauri A, Cescatti A (2021) Emergent vulnerability to climate-driven disturbances in European forests. *Nat Commun* 12(1081):10. <https://doi.org/10.1038/s41467-021-21399-7>

- Gatti RC, Paola AD, Bombelli A, Noce S, Valentini R (2017) Exploring the relationship between canopy height and terrestrial plant diversity. *Plant Ecol* 218:899–908. <https://doi.org/10.1007/s11258-017-0738-6>
- GCOS (2015) Status of the Global Observing System for Climate. WMO, GCOS-195
- Gdulová K, Marešová J, Barták V, Szostak M, Červenka J, Moudrý V (2021) Use of TanDEM-X and SRTM-C data for detection of deforestation caused by bark beetle in Central European Mountains. *Remote Sens* 13(15), <https://doi.org/10.3390/rs13153042>, <https://www.mdpi.com/2072-4292/13/15/3042>
- Geobasis NRW (2022) 3d-messdaten nw. https://www.opengeodata.nrw.de/produkte/geobasis/hm/3dm_1_las/3dm_1_las/. Accessed 23 Feb 2021
- Gruber A, Wessel B, Huber M, Roth A (2012) Operational TanDEM-X DEM calibration and first validation results. *ISPRS J Photogramm Remote Sens* 73:39–49 <https://doi.org/10.1016/j.isprsjprs.2012.06.002>, <http://www.sciencedirect.com/science/article/pii/S0924271612001037>, innovative Applications of SAR Interferometry from modern Satellite Sensors
- Gómez C, Lopez-Sanchez JM, Romero-Puig N, Zhu J, Fu H, He W, Xie Y, Xie Q (2021) Canopy height estimation in Mediterranean forests of Spain with TanDEM-X data. *IEEE J Sel Top Appl Earth Observ Remote Sens* 14:2956–2970. <https://doi.org/10.1109/JSTARS.2021.3060691>
- Herold M, Carter S, Avitabile V, Espejo AB, Jonckheere I, Lucas R, McRoberts RE, Næsset E, Nightingale J, Petersen R, Reiche J, Romijn E, Rosenqvist A, Rozendaal DMA, Seifert FM, Sanz MJ, Sy VD (2019) The role and need for space-based forest biomass-related measurements in environmental management and policy. *Surv Geophys* 40:757–778. <https://doi.org/10.1007/s10712-019-09510-6>
- Hoyo A, Takagi K, Avtar R, Tadono T, Nakamura F (2020) Synthesis of L-Band SAR and forest heights derived from TanDEM-X DEM and 3 digital terrain models for biomass mapping. *Remote Sens*. <https://doi.org/10.3390/rs12030349>, <https://www.mdpi.com/2072-4292/12/3/349>
- Karila K, Vastaranta M, Karjalainen M, Kaasalainen S (2015) TanDEM-X interferometry in the prediction of forest inventory attributes in managed boreal forests. *Remote Sens Environ* 159:259–268 <https://doi.org/10.1016/j.rse.2014.12.012>, <http://www.sciencedirect.com/science/article/pii/S0034425714005045>
- Karila K, Yu X, Vastaranta M, Karjalainen M, Puttonen E, Hyypä J (2019) TanDEM-X digital surface models in boreal forest above-ground biomass change detection. *ISPRS J Photogramm Remote Sens* 148:174–183 <https://doi.org/10.1016/j.isprsjprs.2019.01.002>, <http://www.sciencedirect.com/science/article/pii/S0924271619300024>
- Koch B (2010) Status and future of laser scanning, synthetic aperture radar and hyperspectral remote sensing data for forest biomass assessment. *ISPRS J Photogramm Remote Sens* 65:581–590
- Kugler F, Schulze D, Hajnsek I, Pretzsch H, Papathanassiou K (2014) TanDEM-X Pol-InSAR performance for forest height estimation. *IEEE Trans Geosci Remote Sens* 52(10):6404–6422. <https://doi.org/10.1109/TGRS.2013.2296533>
- Kugler F, Lee SK, Hajnsek I, Papathanassiou KP (2015) Forest height estimation by means of Pol-InSAR data inversion: the role of the vertical wavenumber. *IEEE Trans Geosci Remote Sens* 53(10):5294–5311. <https://doi.org/10.1109/TGRS.2015.2420996>
- Lachaise M, Schweisselhelm B, Fritz T (2020) The new Tandem-X change dem: specifications and interferometric processing. In: 2020 IEEE Latin American GRSS & ISPRS Remote Sensing Conference (LAGIRS), pp 646–651, <https://doi.org/10.1109/LAGIRS48042.2020.9165638>
- Martone M, Braeutigam B, Rizzoli P, Gonzalez C, Bachmann M, Krieger G (2012) Coherence evaluation of TanDEM-X interferometric data. *ISPRS J Photogramm Remote Sens* 73:21–29 <https://doi.org/10.1016/j.isprsjprs.2012.06.006>, <http://www.sciencedirect.com/science/article/pii/S0924271612001207>
- Olesk A, Praks J, Antropov O, Zalite K, Arumae T, Voormansik K (2016) Interferometric SAR coherence models for characterization of Hemiboreal forests using TanDEM-X data. *Remote Sens* 8(700):1–23
- Pan Y, Birdsey RA, Fang J, Houghton R, Kauppi PE, Kurz WA, Phillips OL, Shvidenko A, Lewis SL, Canadell JG, Ciais P, Jackson RB, Pacala SW, McGuire AD, Piao S, Rautiainen A, Sitch S, Hayes D (2011) A large and persistent carbon sink in the world's forests. *Science* 333(6045):988–993 <https://doi.org/10.1126/science.1201609>, <http://science.sciencemag.org/content/333/6045/988>
- Perko R, Raggam H, Deutscher J, Gutjahr K, Schardt M (2011) Forest assessment using high resolution SAR data in X-band. *Remote Sens* 3(4):792–815 <https://doi.org/10.3390/rs3040792>, <http://www.mdpi.com/2072-4292/3/4/792/>
- Rizzoli P, Martone M, Gonzalez C, Wecklich C, Tridon DB, Bräutigam B, Bachmann M, Schulze D, Fritz T, Huber M, Wessel B, Krieger G, Zink M, Moreira A (2017) Generation and performance assessment of the global TanDEM-X digital elevation model. *ISPRS J Photogramm Remote Sens* 132:119–139 <https://doi.org/10.1016/j.isprsjprs.2017.08.008>, <http://www.sciencedirect.com/science/article/pii/S092427161730093X>
- Rizzoli P, Dell'Amore L, Bueso-Bello JL, Gollin N, Carcereri D, Martone M (2022) On the derivation of volume decorrelation from TanDEM-X bistatic coherence. *IEEE J Sel Top Appl Earth Observ Remote Sens* 15:3504–3518. <https://doi.org/10.1109/JSTARS.2022.3170076>
- Rossi C, Rodriguez Gonzalez F, Fritz T, Yague-Martinez N, Eineder M (2012) TanDEM-X calibrated Raw DEM generation. *ISPRS J Photogramm Remote Sens* 73:12–20 <https://doi.org/10.1016/j.isprsjprs.2012.05.014>, <http://www.sciencedirect.com/science/article/pii/S0924271612001062>, innovative Applications of SAR Interferometry from modern Satellite Sensors
- Sadeghi Y, St-Onge B, Leblon B, Simard M (2016) Canopy height model (CHM) derived from a TanDEM-X InSAR DSM and an airborne lidar DTM in boreal forest. *IEEE J Sel Top Appl Earth Observ Remote Sens* 9(1):381–397. <https://doi.org/10.1109/JSTARS.2015.2512230>
- Schlund M, Baron D, Magdon P, Erasmi S (2019a) Canopy penetration depth estimation with TanDEM-X and its compensation in temperate forests. *ISPRS J Photogramm Remote Sens* 147:232–241 <https://doi.org/10.1016/j.isprsjprs.2018.11.021>, <http://www.sciencedirect.com/science/article/pii/S0924271618303228>
- Schlund M, Magdon P, Eaton B, Aumann C, Erasmi S (2019b) Canopy height estimation with TanDEM-X in temperate and boreal forests. *Int J Appl Earth Observ Geoinform* 82:101904 <https://doi.org/10.1016/j.jag.2019.101904>, <http://www.sciencedirect.com/science/article/pii/S0303243418311577>
- Schlund M, Erasmi S, Scipal K (2020) Comparison of aboveground biomass estimation from InSAR and LiDAR canopy height models in tropical forests. *IEEE Geosci Remote Sens Lett* 17(3):367–371. <https://doi.org/10.1109/LGRS.2019.2925901>
- Schlund M, Kotowska MM, Brambach F, Hein J, Wessel B, Camarretta N, Silalahi M, Surati Jaya IN, Erasmi S, Leuschner C, Krefth H (2021) Spaceborne height models reveal above ground biomass changes in tropical landscapes. *For Ecol Manag* 497:119497 <https://doi.org/10.1016/j.foreco.2021.119497>, <https://www.sciencedirect.com/science/article/pii/S0378112721005879>
- Schweisselhelm B, Lachaise M, Fritz T (2020) An adaptive filtering approach for the new TanDEM-X Change DEM. In: IGARSS 2020—2020 IEEE International Geoscience and Remote Sensing Symposium, pp 3416–3419. <https://doi.org/10.1109/IGARS539084.2020.9323369>

- Seidl R, Schelhaas MJ, Rammer W, Verkerk PJ (2014) Increasing forest disturbances in Europe and their impact on carbon storage. *Nat Clim Change* 4:806–810. <https://doi.org/10.1038/nclimate2318>
- Skidmore AK, Coops NC, Neinavaz E, Ali A, Schaepman ME, Paganini M, Kissling WD, Vihervaara P, Darvishzadeh R, Feilhauer H, Fernandez M, Fernández N, Gorelick N, Geijzendorffer I, Heiden U, Heurich M, Hobern D, Holzwarth S, MullerKarger FE, Kerchova RVD, Lausch A, Leitao PJ, M C Lock CAM, O'Connor B, Rocchini D, Roquesli C, Turner W, Vis JK, Wang T, Wegmann M, Wingate V, (2021) Priority list of biodiversity metrics to observe from space. *Nat Ecol Evol* 5:896–906. <https://doi.org/10.1038/s41559-021-01451-x>
- Solberg S, Astrup R, Weydahl DJ (2013) Detection of forest clear-cuts with shuttle radar topography mission (SRTM) and Tandem-X InSAR data. *Remote Sens* 5(11):5449–5462 <https://doi.org/10.3390/rs5115449>, <http://www.mdpi.com/2072-4292/5/11/5449>
- Solberg S, Naesset E, Gobakken T, Bollandsas OM (2014) Forest biomass change estimated from height change in interferometric SAR height models. *Carbon Balance Manag* 9(1):5. <https://doi.org/10.1186/s13021-014-0005-2>
- Solberg S, Hansen EH, Gobakken T, Naesset E, Zahabu E (2017) Biomass and InSAR height relationship in a dense tropical forest. *Remote Sens Environ* 192:166–175 <https://doi.org/10.1016/j.rse.2017.02.010>, <http://www.sciencedirect.com/science/article/pii/S0034425717300603>
- Solberg S, May J, Bogren W, Breidenbach J, Torp T, Gizachew B (2018) Interferometric SAR DEMs for Forest Change in Uganda 2000–2012. *Remote Sens* 10(2):1–17. <https://doi.org/10.3390/rs10020228>
- Tanase MA, Ismail I, Lowell K, Karyanto O, Santoro M (2015) Detecting and quantifying forest change: the potential of existing C- and X-band radar datasets. *PLoS One* 10(6):1–14. <https://doi.org/10.1371/journal.pone.0131079>
- Thüringer Landesamt für Bodenmanagement und Geoinformation (TLBG) (2022) Höhendaten von 2014 bis 2019. <https://www.geoportal-th.de/de-de/Downloadbereiche/Download-Offene-Geodaten-Thüringen/Download-Höhendaten>. Accessed 23 Feb 2021
- Tian J, Schneider T, Straub C, Kugler F, Reinartz P (2017) Exploring digital surface models from nine different sensors for forest monitoring and change detection. *Remote Sens* 9(3):287. <https://www.mdpi.com/2072-4292/9/3/287>
- Ullah S, Dees M, Datta P, Adler P, Saeed T, Khan MS, Koch B (2020) Comparing the potential of stereo aerial photographs, stereo very high-resolution satellite images, and TanDEM-X for estimating forest height. *Int J Remote Sens* 41(18):6976–6992. <https://doi.org/10.1080/01431161.2020.1752414>
- Wang H, Fu H, Zhu J, Liu Z, Zhang B, Wang C, Li Z, Hu J, Yu Y (2021) Estimation of subcanopy topography based on single-baseline TanDEM-X InSAR data. *J Geodesy* 95(84):1–19. <https://doi.org/10.1007/s00190-021-01519-3>
- Wessel B, Huber M, Wohlfart C, Marschalk U, Kosmann D, Roth A (2018) Accuracy assessment of the global TanDEM-X digital elevation model with GPS data. *ISPRS J Photogramm Remote Sens* 139:171–182. <https://doi.org/10.1016/j.isprsjprs.2018.02.017>, <http://www.sciencedirect.com/science/article/pii/S0924271618300522>
- Wessel B, Lachaise M, Bachmann M, Schweisshelm B, Huber M, Fritz T, Tubbesing R, Buckreuss S (2022) The new TanDEM-X DEM 2020: generation and specifications. In: *EUSAR 2022; 14th European Conference on Synthetic Aperture Radar*, pp 25–29